PAPER • **OPEN ACCESS**

Effect of structure and texture on failure of pipe steel sheets produced by TMCP

To cite this article: M L Lobanov *et al* 2020 *IOP Conf. Ser.: Mater. Sci. Eng.* **709** 044010

IOP Conf. Series: Materials Science and Engineering **709** (2020) 044010 doi:10.1088/1757-899X/709/4/044010

Effect of structure and texture on failure of pipe steel sheets produced by TMCP

M L Lobanov[1,2], S V Danilov[1,*] and V N Urtsev[3]

[1]Ural Federal University, Yekaterinburg, Russia
[2]Institute of Metal Physics, Ural Branch of RAS, Yekaterinburg, Russia
[3]Ausferr Research and Technology Center, Magnitogorsk, Russia

* s.v.danilov@bk.ru

Abstract. The method of orientation microscopy (EBSD) is used to study the structure and texture of low-carbon, low-alloy pipe steel sheets processed by controlled thermomechanical processing (TMCP). The temperatures of isothermal hot rolling varied. Samples cut from sheets showed a different properties during mechanical testing. The formation of cleavages (secondary cracks) during failure of steel is related to the presence of ferrite grains with orientation {001}<110> extended in the hot rolling direction. The formation of grains is a consequence of the isothermal hot rolling below the temperature Ac_3 at TMCP.

1. Introduction

An increase in working pressure as a result of using high-strength steels is one of the most promising ways of increasing the economic efficiency of main gas pipelines located in complex climatic conditions. The obvious advantage of using high-strength pipes is a reduction in metal content (pipe wall thickness). The breakthrough in improvement of structural strength of low-alloy pipe steels occurred in the middle of the 1970s in view of the development and introduction into industrial production of thermomechanical controlled processing (TMCP) combining controlled rolling and subsequent controlled cooling [1–3].

Research in recent years has shown that a feature of bainitic steels of strength classes X70 and X80 is the critical role of formation within a fracture (during tensile, impact bending, static crack resistance tests) of secondary cracks, i.e., cleavages, propagating perpendicular to the main crack plane. It is important to note that separations are observed in contemporary large diameter pipes (LDP) with ductile crack propagation [4, 5]. On the example of contemporary pipe steels with low contamination by inclusions and quite uniform microstructure, it has been demonstrated that cleavages are caused by features of microstructure formed during sheet treatment [4, 5], which determines their strict orientation along the rolling direction (RD). In [5–7], reasons for forming cleavages in high-strength pipe steels with a bainitic structure, low content of carbon and harmful impurities are also connected with preferred crystallographic texture. In the destruction of pipe steel sheets, an important role is played not by the integral texture but by a single weak component (001)[110], as shown in [7–10]. Crack development depends on the presence of extended regions with consistent orientation over a distance exceeding the critical crack size.

In the present work, we investigate the formation of structural and textural states in sheets of low-carbon, low-alloy pipe steel obtained by TMCP depending on isothermal hot rolling temperatures.

2. Research methods

We investigate sheet samples (depth 27 mm) of 06G2MB low-carbon, low-alloy pipe steel, containing 0.06 wt % C, 1.7 wt % Mn, ~ 0.05 wt % Nb, and ~ 0.05 wt % Mo, (The remainder is Fe and unavoidable impurities). The isothermal hot rolling temperatures (Ti_{HR}) of steel sheets made up ~ 920 °C (State I), ~ 840 °C (State II) and ~ 760 °C (State III).

Calculations of phase thermodynamic equilibria were carried out using ThermoCalc software. The calculated steel temperature Ac_3 was equal to 830 °C.

The TMCP steel sheets were cut along the RD for mechanical testing. Tests have demonstrated a marked difference between modes I, II and III (table 1).

Table 1. Mechanical properties of the samples of low-carbon low-alloy steels.

State	T_{iHR}, (°C)	Yield strength, (MPa)	Tensile strength, (MPa)	δ_5, (%)	KCV_{-60}, (J/cm^2)	KCV_{-40}, (J/cm^2)	Tendency to cleavage
I	~ 920	480–500	560–570	26.0	230–370	270–330	not observed
II	~ 840	550–560	610–630	23.5	380–400	350–380	not observed
III	~ 760	530–550	590–610	24.5	360–380	300–340	observed

Metallographic sections are prepared from the steel samples in plane defined by the direction of rolling in TMCP and the normal to the rolling plane. The sample structure is investigated electron microscopically by means of a ZEISS CrossBeam AURIGA scanning microscope (with an accelerating voltage of 20 kV). To determine the orientation of individual grains and analyze the local texture, we use an EBSD HKL Inca attachment with an Oxford Instruments analytical system. The scanning increment is 0.1 μm. The error in determining the lattice orientation is no more than ± 1° (± 0.6° on average). Small angle boundaries between the local volumes are plotted on orientation charts when the disorientations are 2–7° and 8–15°; the boundary thickness in the graphics is 1 and 2 pixel. Large-angle boundaries between the local volumes are plotted on orientation charts when the disorientation exceeds 15°; the boundary thickness in the graphics is 3 pixels. The texture is investigated by plotting orientation distribution functions (ODF). Analysis of the special boundaries between individual grains involves plotting such boundaries on orientation charts, in the light of the standard Brandon criterion $\pm \Delta\Theta$ in the software. For each boundary, $\Delta\Theta = 15°/\Sigma n)^{1/2}$, where Σn is the number of coinciding points when three dimensional crystal lattices are superimposed.

In orientation analysis, the laboratory system adopted is the coordinate system whose axes are, respectively, parallel to the direction of hot rolling in TMCP (X||RD), to the normal (ND) to the rolling plane (Y||ND), and to the perpendicular direction (TD) that runs along the roller axis (Z||TD). Accordingly, these three directions form a right triad of vectors.

3. Results and discussion

In the samples II with bainite structure after TMCP (figures 1, b; 2, b), we observe extended regions that run in the direction of rolling (thickness 5–35 μm). These regions correspond to austenite grains deformed by controlled rolling. They have taken on bainite structure as a result of $\gamma \rightarrow \alpha$ transition. Presumably, the dimensions of the regions corresponding to the initial austenite grains are retained on account of the formation of disperse carbides at the boundaries in hot deformation [1]. In the samples III after TMCP (figures 1, c; 2, c), we observe extended regions with practically parallel boundaries that run in the direction of rolling (thickness 5–25 μm). Elongated ferrite phase grains (thickness to 5 μm) were observed in the samples III after TMCP along the boundaries of the initial deformed γ-grains (figures 1, c; 2, c). This ferrite can be identified as high temperature α-phase existed in steel by isothermal hot rolling. Some α-grains were fragmented. They had time recrystallization. Equations should be centred and should be numbered with the number on the right-hand side.

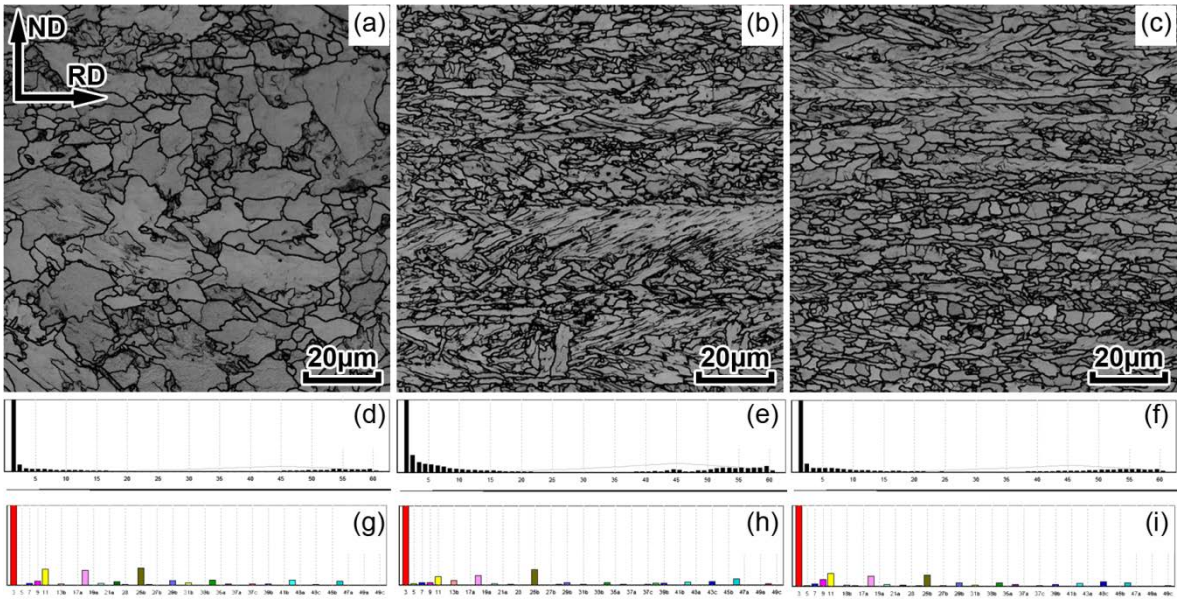

Figure 1. The microstructure of the steel in the TMCP states in the form of orientation maps (EBSD) – band contrast and intercrystalline boundaries: (a), (d), (g) – I; (b), (e), (h) – II; (c), (f), (i) – III; (d), (e), (f) – distribution of intercrystalline boundaries; (g), (h), (i) – distribution of CSL boundaries.

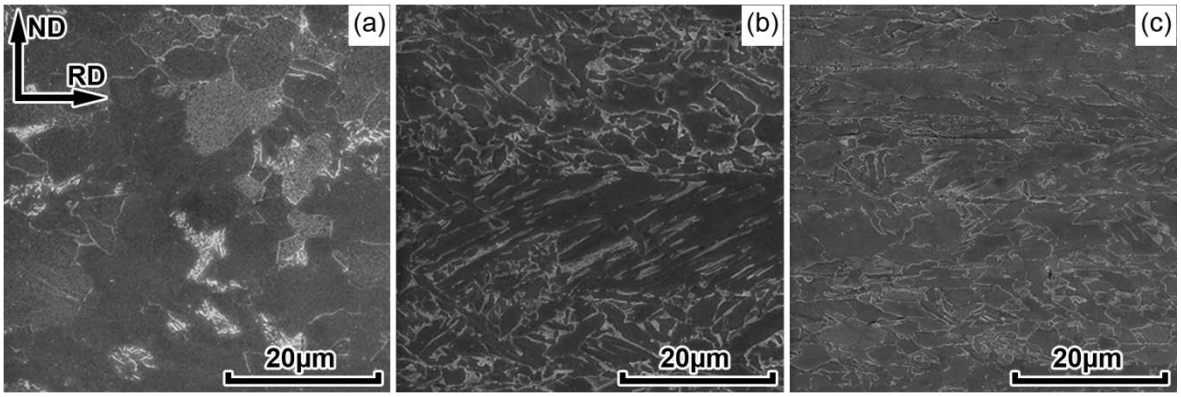

Figure 2. The microstructure of the steel in the TMCP states (image in swallowed up electrons): (a) – I; (b) – II, (c) – III.

In sample 1, the main volume was occupied by large bainite grains (figures 1, a; 2, a) of non-equilibrium shape and with the maximum size up to 35 microns. The elongation of the grain shape in the direction of RD was not observed. Obviously, austenite underwent recrystallization from the end of hot deformation to the start of accelerated cooling. A small part of the volume is occupied by "bright" areas that have their own structure (figure 2, a). It is clear that these areas under a larger magnification are tempered lamellar martensite with carbides at the intercrystalline boundaries.

All large-angle boundaries are concentrated with disorientations of 49–60° (figure 1, d, e, f). In the spectra of special boundaries observed in all structures, boundaries of the coincidence site lattices (CSL): Σ3, Σ11, Σ17b, Σ25b, Σ33c, and Σ41c are the most strongly expressed (figure 1, g, h, i). This spectrum is the result of shear phase transformation, in accordance with orientation relations (OR) intermediate between the Kurdjumov–Sachs (K-S) and Nishiyama–Wasserman types, as shown in [11]. Such spectra of special boundaries are also seen in the martensite of low-carbon pipe steel [12, 13].

EBSD data show that the texture of II and III the samples consists mainly of the same scattered components: very strong (001)[110] orientations, two ~ {112}<110> orientations, and two ~ {110}<223> (figure 3, c, d, e, f). In the samples III the (001)[110] orientation and the {112}<110> orientations expressed more strongly (figure 3, c, e). The main orientations correspond to relatively uniform regions consisting of crystallites separated by small-angle boundaries.

The crystallographic texture of sample I had the following features: 1) large scattering of the main orientations, 2) a certain deviation of the crystallographic axes around which scattering occurs (figure 3, a, b). An analysis of the crystallographic relationship between the α-phase orientations and possible austenite orientations through the K-S OR showed that α-phase grains were formed in recrystallized γ-phase grains with the <100> axis parallel to RD. Obviously due to the high temperature of the end of hot deformation in mode I, the γ-phase recrystallized during the residence from the end of rolling to the start of accelerated cooling.

The applied orientational EBSD technique allowed to define the structurally ferrite in the samples III and analyse the texture. All indicated orientations of the ferrite formed at hot rolling, namely: {001}<110>, {11k}<110>, are stable deformation orientations of the BCC lattice [14]. It should be noted that, taking into account the crystal-geometric characteristics of structurally ferrite (orientation, shape and size of grains), it can be considered as a kind of "macro defect". Propagation of longitudinal cracks will be predetermined in the crystallographic planes {001} of elongated ferrite grains [8–10, 15].

Obviously, the elongated ferritic grains formed during isothermal hot rolling at temperatures below Ac_3. It is also obvious that they are the cause of reduction in mechanical properties.

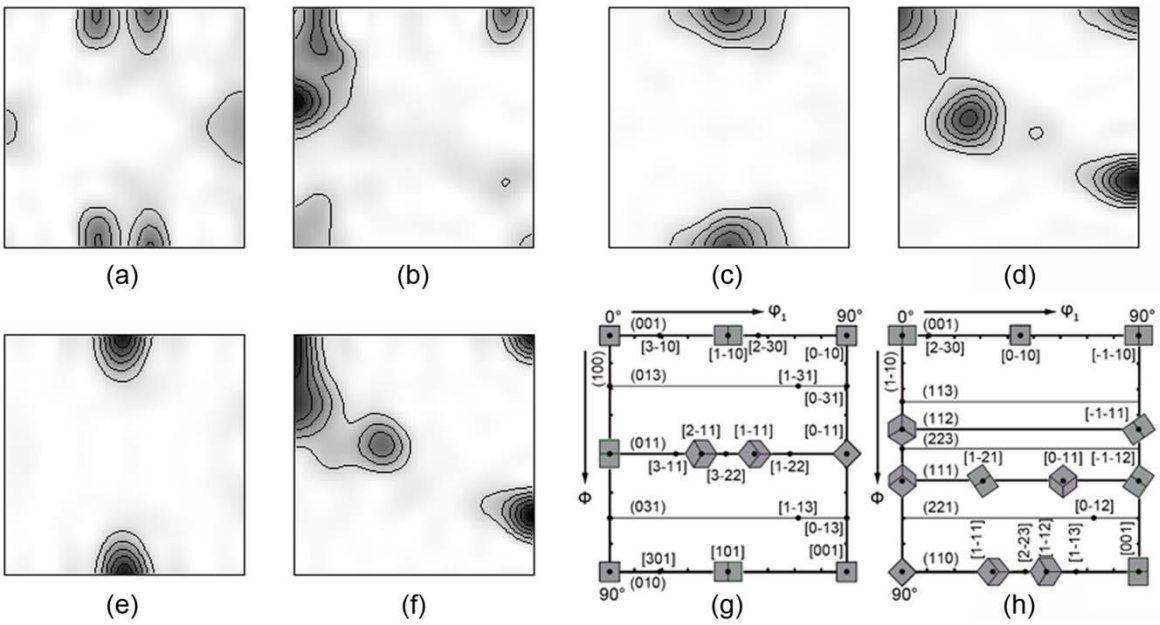

Figure 3. The texture of the steel in the TMCP I (a, b) II (c, d) and III (e, f) as ODF sections: (a), (c), (e), (g) – sections φ2 = 0°; (b), (d), (f), (h) – sections φ2 = 45°; (g), (h) – schematic orientations from the direction perpendicular to the RD-ND plane on ODF sections.

4. Summary

The formation of cleavages the destruction of low-carbon low-alloy steel pipe with a bainitic structure obtained controlled thermo-mechanical treatment, due to the presence in the material of the crystallographic texture components (001)[110] and {11k}<110>. The elongated ferritic grains the region with uniform orientation of the (001)<110> and {11k}<110> formed during isothermal hot rolling by TMCP at temperatures below Ac_3.

Acknowledgments
The work was carried out using the laboratory equipment "Structural methods of analysis and properties of materials and nanomaterials" of the Center of Ural Federal University. Authors are grateful for the assistance the program of support for leading universities in Russian Federation for improvement of their competitiveness No 211 of the Government No 02.A03.21.0006. The authors thank MMK company for support and assistance in organizing the study.

References
[1] Hulka K, Peters P and Haisterkamp F 1992 *Steel Transl.* **27** 64–70
[2] Zhao M -C, Yang K and Shan Y 2002 *Mater. Sci. Eng., A* **335** 14–20
[3] Endo S and Nakata N 2015 *JFE Technical Report* **20** 1–7
[4] Mannucci G and Demofonti G 2011 *The Journal of Pipeline Engineering* **10** 133–45
[5] Chatterjee S, Koley S, Das Bakshi S and Shome M S 2017 *Mater. Sci. Eng., A* **708** 254–66
[6] Hara T, Asahi H, Shinohara Y and Terada Y 2006 *Proc. of the Biennial Int. Pipeline Conf., IPC* (Calgary: ASME) pp 245–50
[7] Sasidhar K N, Dhande T, Javed N, Ghosh A, Mukherjee M, Sharma V, Mahashabde V V and Das Bakshi S 2017 *Mater. Des.* **128** 86–97
[8] Pyshmintsev I Y, Struin A O, Gervasyev A M, Lobanov M L, Rusakov G M, Danilov S V and Arabey A B 2016 *Metallurgist* **60** 405–12
[9] Pyshmintsev I, Gervasyev A, Petrov R H, Olalla V C and Kestens L 2012 *Mater. Sci. Forum* **702–703** 770–73
[10] Mohtadi-Bonab M A, Eskandari M and Szpunar J A 2014 *Mater. Sci. Eng., A* **620** 97–106
[11] Lobanov M L, Rusakov G M, Redikul'tsev A A, Belikov S V, Karabanalov M S, Struina E R and Gervas'ev A M 2016 *Phys. Met. Metallogr.* **117** 254–59
[12] Stepanov A I, Ashikhmina I N, Sergeeva K I, Belikov S V, Musikhin S A, Karabanalov M S and Al-Katawi A A 2014 *Steel Transl.* **44** 469–73
[13] Lobanov M L, Borodina M D, Danilov S V, Pyshmintsev I Y and Struin A O 2017 *Steel Transl.* **47** 710–16
[14] Hölscher M, Raabe D and Lücke K 1994 *Acta Metallurgica Et Materialia* **42** 879–86
[15] Pyshmintsev I U, Veselov I N, Yakovleva A A, Lobanov M L and Danilov S V 2016 *AIP Conf. Proc.* **1785** 040053